Microfluid Nanofluid (2010) 9:163–170
DOI 10.1007/s10404-009-0509-3

RESEARCH PAPER

Fabrication of high-aspect-ratio polymer nanochannels using a novel Si nanoimprint mold and solvent-assisted sealing

Y. H. Cho · J. Park · H. Park · X. Cheng · B. J. Kim · A. Han

Received: 7 July 2009 / Accepted: 14 September 2009 / Published online: 19 November 2009
© Springer-Verlag 2009

Abstract We present a low cost nanofabrication method to fabricate high-aspect-ratio (HAR) polymer nanochannels using a novel silicon nanoimprint mold fabrication technique and a solvent-assisted sealing method. These nanofluidic channels are being developed for single biomolecule detection. The silicon nanoimprint mold fabrication process is based on the combination of anisotropic etching of silicon by potassium hydroxide (KOH) solution and the local oxidation of silicon (LOCOS) process. The resulting high-aspect-ratio silicon mold has smooth sidewalls owing to the anisotropic KOH etching process along the silicon crystalline geometry as well as the LOCOS process. The nanostructures in the nanoimprint molds that form the nanochannels can be easily controlled by the initial micropattern sizes defined using conventional UV lithography and the oxidation time, making this technique a practical solution for low cost and high-throughput HAR silicon nanoimprint mold fabrication. Nanoimprint molds having aspect ratios of more than 1:5.5 (width: 200 nm, height: 1.1 μm, length: 1 cm) were successfully fabricated. Nanoimprinting technique was used to create poly(methyl methacrylate) (PMMA) nanotrenches out of this nanoimprint mold. A novel solvent-assisted sealing technique was developed in order to seal the HAR PMMA nanotrenches. This technique enables the generation of nanochannels with various nanoscale dimensions without the need for complicated and expensive nanolithography tools.

Keywords Nanochannel fabrication · Nanoimprint lithography · High-aspect-ratio nanostructure

Y. H. Cho
School of Mechanical Design and Automation Engineering, Seoul National University of Technology, Seoul, Korea

J. Park · H. Park · X. Cheng · A. Han (✉)
Department of Electrical and Computer Engineering, Texas A&M University, 235G WERC, TAMU 3128, College Station, TX 77843-3128, USA
e-mail: arum.han@ece.tamu.edu

B. J. Kim
CIRMM, Institute of Industrial Science, The University of Tokyo, Tokyo, Japan

1 Introduction

Nanofluidic devices enable isolation, manipulation, and analysis of single biomolecules such as DNA and proteins, essential functions in the newly emerging field of nanobiotechnology (Huh et al. 2007; Craighead 2006; Tegenfeldt et al. 2004; Jo et al. 2007; Mannion et al. 2006). The radius of gyration of DNA ($\sim$400 nm) begins to match with the dimensions of nanofluidic channels, making nanochannels as one of the most effective tools for manipulating and analyzing the behaviors and movements of a single DNA strand (Jo et al. 2007; Mannion et al. 2006). Consequently, various fabrication techniques have been developed to meet the increasing demand for nanofluidic devices, including nanochannels (Abgrall and Nguyen 2008; Perry and Kandlikar 2006).

Top-down nanolithography such as focused ion beam (FIB) milling (Wang et al. 2006; Riehn et al. 2005), e-beam lithography (EBL) (Mannion et al. 2006; Tamaki et al. 2006), and scanning probe patterning (Mikayama et al. 2005) are some of the most straightforward methods to directly fabricate nanochannels. Despite their high-resolution nanofabrication capabilities, they suffer from low throughput and high cost, making those techniques not suitable for mass production of nanofluidic devices. Being

able to perform repeated and well-controlled nanofluidic experiments require a large number of devices because nanofluidic devices are sensitive to contamination and difficult to clean, making it hard to re-use.

Nanoimprint lithography (NIL) is one of the most promising technologies for low cost and high-throughput patterning of nanoscale features over a large area (Tegenfeldt et al. 2004; Chou et al. 1996; Cao et al. 2002; Guo et al. 2004; Dumond et al. 2006; Reano and Pang 2005). In NIL, an imprinting master template-containing nanoscale structures are directly replicated onto polymer substrates or resists repeatedly. Therefore, fabricating a high-resolution imprinting master is critical, typically requiring high-resolution nanolithography. The most common methods in nanoimprinting mold fabrications are to use top-down nanolithography technologies such as EBL (Tamaki et al. 2006) and FIB milling (Langford et al. 2007) on silicon or quartz substrates. Although extremely well-defined nanostructures can be easily obtained using these techniques, the fabrication cost is high. Alternatively, methods such as edge lithography have been developed for NIL stamp fabrication, which utilizes selective removal or deposition of materials at the edges of lithographically defined microscale features (Grabiec et al. 2004; Haneveld et al. 2006; Zaborowsk et al. 2006; Zhao et al. 2008; Liang et al. 2007; Chen et al. 2007). For example, Grabiec et al. demonstrated the use of local oxidation of silicon (LOCOS) for NIL stamp fabrication (Grabiec et al. 2004). Although the stamp widths and lengths could be easily controlled by this technique, a single stamp could only contain a single pattern width controlled by the oxidation time. Also, level differences on both sides of the nanostructures occurred due to the differences in etching time, resulting in non-uniform height as well as making nanotrench sealing a difficulty. Another approach like shadow edge lithography (SEL) to fabricate nanochannels using the shadow effect has been reported (Bai et al. 2007, 2009). This method offered both good resolution and high throughput, but the mold had high surface roughness.

For many applications requiring high flow rate and/or pressure-driven flow, high-aspect-ratio (HAR) nanochannels would be an optimal choice (Abgrall and Nguyen 2008). Low cost fabrication methods based on SiO_2 imprinting mold as mentioned above could be used, but the molds are typically not mechanically strong enough compared to Si stamps, making HAR SiO_2 nanoimprint molds easy to break during the imprinting process (Grabiec et al. 2004).

We have previously reported the fabrication of silicon dioxide nanochannel arrays using bulk micromachining without using nanolithography (Cho et al. 2007). Here, we present a simple method to fabricate HAR poly(methyl methacrylate) (PMMA) nanochannel arrays by utilizing a variation of previously developed SiO_2 nanochannel fabrication technique and combining it with a novel solvent-assisted sealing method. Our nanoimprinting mold fabrication technique allows nanostructure dimensions to be precisely and easily controlled by conventional optical lithography micropatterns and thermal oxidation processing conditions. Thus, we can easily fabricate HAR nanotrench arrays having various widths on the same device by simply starting with micropatterns of different widths.

In nanochannel fabrication, one of the main challenges is sealing the nanochannels with a cover layer with sufficient bond strength but without the cover layer collapsing or sagging into the channels that can cause channel blockage. Our newly developed solvent-assisted sealing technique overcomes such limitations by directly sealing HAR polymer nanotrenches by exposing the nanochannels to solvent vapor. Due to the HAR nanotrench geometry, only the topsides of the nanotrenches were affected by solvent vapor and were sealed. The fabricated nanochannels were used for DNA stretching experiments inside the nanochannels. It is expected that this simple nanochannel fabrication technique can provide means for low cost and high-throughput polymer nanochannel fabrication.

2 Methods

2.1 Silicon nanoimprint mold fabrication

Figure 1 shows the fabrication steps for the silicon nanoimprint mold using a 3-inch <100> oriented single crystalline silicon wafer. First, a 100 nm thick silicon nitride (Si_3N_4) layer serving as an etch mask for KOH etching of silicon was deposited by low-pressure chemical vapor deposition (LPCVD, SAMCO, Japan) (Fig. 1a). Next, the line patterns of the Si_3N_4 layer was formed 45° to the primary flat of the Si wafer (Fig. 1f) by standard photolithography and reactive ion etching (RIE) (March Plasma Systems Model CS-1701, 50 sccm CF_4 gas, 75 W, 65 mTorr) (Fig. 1b, f). After RIE, no delay in Si etching was observed when removing the natural SiO_2 layer using BOE. To find the <100> crystallographic line that could be used as an alignment mark (<100> direction), small V-groove lines were formed using a brief KOH etching (40 wt%, 80°C for 5 min) before the main KOH etching step (Vangbo and Backlund 1996). The widths of the patterned lines were 2.5–3.0 μm and played an important role in determining the final widths and heights of the nanostructures on the nanoimprinting mold. The exposed Si layer was anisotropically etched in KOH solution (40 wt%, 56°C for 3 min) resulting in silicon structures with vertical side walls due to the relatively lower etching rate of <100> surface of the single crystal silicon wafer (Fig. 1c). The

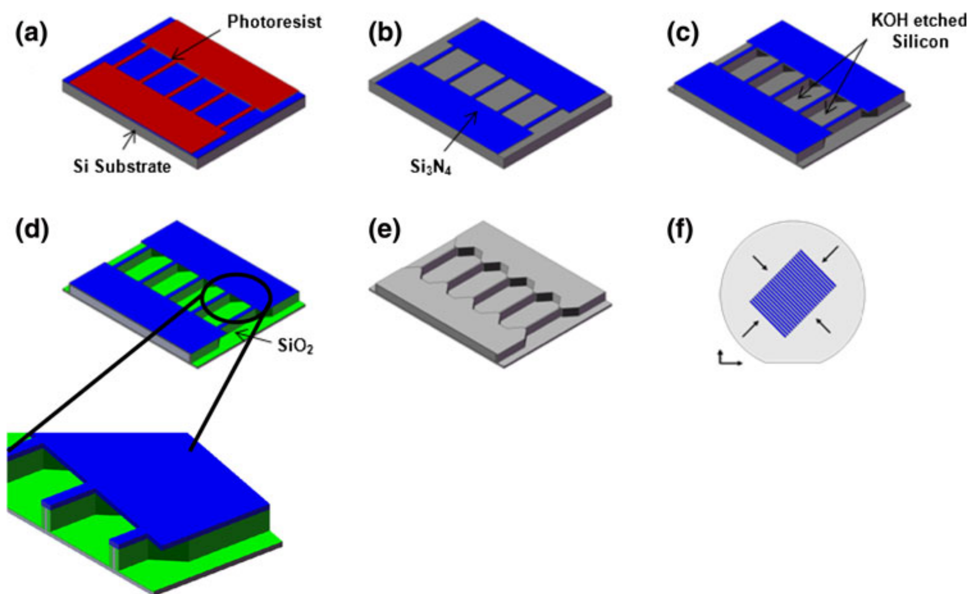

Fig. 1 Silicon nanoimprint mold fabrication steps. **a** Si_3N_4 deposition and photolithography, **b** RIE of Si_3N_4, **c** Anisotropic Si etching using KOH solution resulting in vertical Si structures, **d** Local oxidation of silicon (LOCOS), **e** HF wet etching and RIE for SiO_2 and Si_3N_4 layers removal, **f** Illustration showing the top side view of the pattern alignment scheme for anisotropic Si etching in KOH solution

etch rates of Si <100> planes in 40 wt% KOH, 56°C was 0.3 μm/min. The KOH etch time determines the final height of the nanostructure. LOCOS was then performed using an oxidation furnace at 1,100°C for 4 h in order to consume Si to a final thickness of 200–500 nm (Fig. 1d). This oxidation time determines the final width of the nanostructure. Finally, the SiO_2 layers were immediately removed by HF wet etching and Si_3N_4 layers were removed by RIE (50 sccm CF_4 gas, 75 W, 65 mTorr) and HF wet etching (over 6 min) (Fig. 1e).

2.2 Nanoimprint lithography for high-aspect-ratio nanotrench fabrication

PMMA is a commonly used polymer resist in NIL and has good optical clarity. The material also has low auto fluorescence, which minimizes background noise in fluorescence based molecular detection. The imprinting molds from the previous fabrication steps were first coated with 1H,1H,2H,2H-perfluorodecyltrichlorosilane (FDTS, Gelest, Inc., Morrisville, PA) for anti-stiction and easy mold release (Nishino et al. 1999). Two kinds of PMMA substrates were used for nanoimprinting. One substrate was a Si substrate having a 930 nm thick spin-coated PMMA resist on it (M.W. = 75,000, Scientific Polymer Products, Inc., Ontario, NY) and the other was a commercially obtained 1.5 mm thick PMMA plate (M.W. = 100,000, T_g = 105°C, Plexiglas®, Philadelphia, PA). The imprinting step was carried out at 175°C and 5×10^6 Pa for 5 min (Specac 15 Ton Manual Hydraulic Press, Specac Ltd, London, UK) (Fig. 2a, b). The temperature distribution of the hydraulic press was uniform throughout the 100 mm diameter platen used as pressing surfaces. The temperature of the platens was controlled by an automatic digital temperature controller, resulting in stability of ±1.0°C. The rising and the cooling times and rates did not affected the imprinting results. After imprinting, the substrate was cooled down to 60°C and the substrate and mold were manually separated. To make the imprinted PMMA structures hydrophilic, an oxygen plasma treatment step was carried out for 2 min (Plasma Cleaner, Harrick Plasma, Ithaca, NY). The power and flow rate of O_2 plasma we used here was 29.6 W and 20 sccm, which was a very low-power one mainly used for surface hydrophilic treatment and no capability of actually etching a polymer.

2.3 Solvent-assisted nanochannel sealing

To create nanochannel structures from the imprinted PMMA nanotrenches, a sealing process is required. We developed a solvent-assisted sealing technique to seal the PMMA nanotrenches. PMMA nanotrenches created from the HAR nanoimprint mold was exposed to either toluene (anhydrous, 99.8%, Sigma-Aldrich, St. Louis, MO) or methanol (EMD Chemicals, Inc., Gibbstown, NJ) vapor for 10–15 s in order to chemically melt the top part of the nanotrenches (Fig. 2c). As shown in Fig. 2e–i, during solvent sealing, micro-reservoirs for inlet and outlet were covered with PDMS sheets. Toluene and methanol were boiled on a hotplate at 250 and 100°C, respectively, to create vapor. The HAR geometry allows only the top part of the nanotrenches to react with solvent vapor while leaving the bottom part of the nanotrenches undamaged. This resulted in the top part of the trenches to melt and collapse, thereby forming nanochannel structures (Fig. 2d).

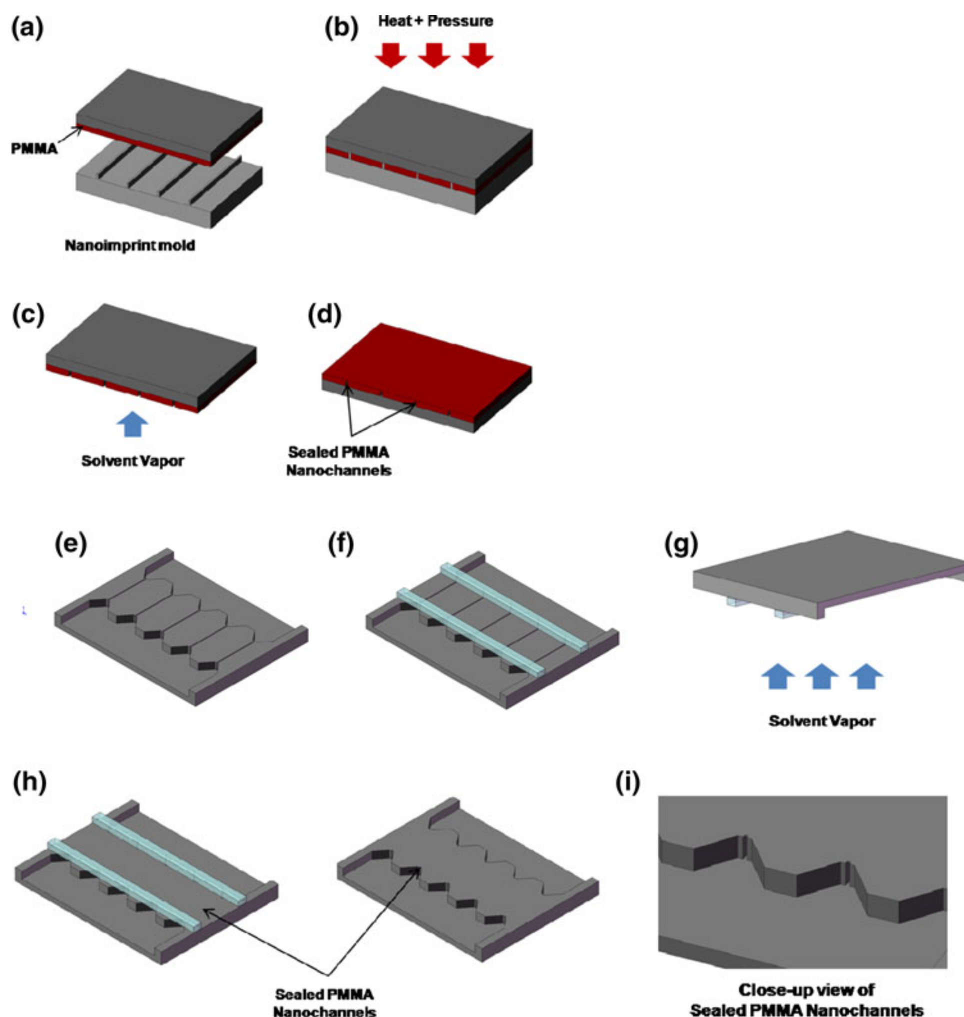

Fig. 2 Illustration showing the PMMA nanochannel fabrication steps using nanoimprinting and solvent-assisted sealing of nanochannels. **a**–**b** PMMA spin-coated on a blank wafer is pressed against the nanoimprint mold. **c**–**d** PMMA nanotrenches are exposed to toluene vapor to obtain sealed nanochannels. **e**–**i** Sealing of nanotrenches with micro-revervoirs on PMMA plate

2.4 DNA loading into nanochannels

DNA loading experiments were conducted as described in our previous publication (Cho et al. 2007). Briefly, capillary force was used to load the DNA into the nanochannel without using any external electrokinetic flow. The nanochannel array was mounted on an x–y translational stage located on an upright fluorescent microscope (Eclipse LV 100D, Nikon America Inc., Melville, NY) equipped with an oil-immersion 100× objective lens (N.A. = 1.40). The flow in the nanochannel was imaged by a digital camera (DS-2Mv, Nikon America Inc., Melville, NY) mounted on the microscope.

3 Results and discussions

3.1 Fabricated silicon nanoimprint mold

By employing bulk micromachining without nanolithography, we successfully fabricated HAR Si nanoimprint molds from <100> oriented silicon wafers. Figure 3 shows scanning electron microscopy (SEM) images of the fabricated silicon nanoimprint structures having widths ranging from 500 nm down to 100 nm with height of 1.1 μm. The initial microscale pattern sizes from the photomask, KOH etching time, and LOCOS time resulted in these specific dimensions. Therefore, by controlling the KOH etching time and the LOCOS time, or by starting with a smaller initial pattern sizes, smaller structures or structures with desired feature sizes can be obtained. Figure 3a shows an example of the resulting HAR silicon nanoimprint mold having widths of 200 nm and heights of 1.1 μm (aspect ratio 1:5.5). Since the nanoimprint mold sections were cut 45° to the pattern orientation, the actual size of the mold was 1.4 times smaller (cos 45°) than that of the SEM images shown in Fig. 3a. Uniformity of the nanoimprint mold was analyzed from a 2 cm × 2 cm Si wafer having 550 nanoridges with 11 different pattern widths. The smallest nanoridges had an average width of 200 ± 10 nm ($n = 10$) and the largest nanoridges had an average width of 500 ± 15 nm ($n = 10$). All other nanoridges also had

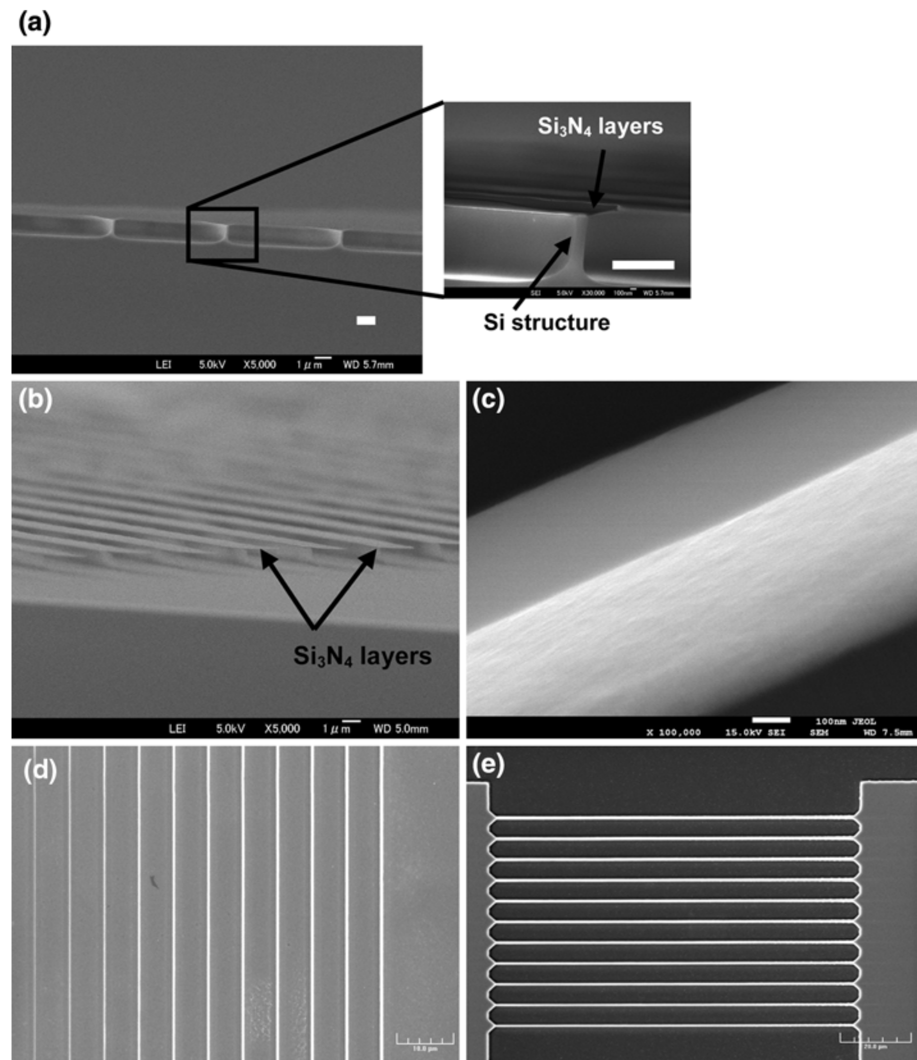

Fig. 3 SEM images of a HAR Si nanoimprint molds. **a** Width and height of the Si structures are 200 nm and 1.1 μm, respectively. Scale bar: 1 μm. **b** Si_3N_4 layers on Si structures. **c** Close-up view of the side-walls after removing Si_3N_4 layer. **d** Si structures with different width ranging from 100 to 500 nm (*bottom to top*). **e** Si mold with micro-reservoir on both side of the nanoridges. Lengths of nanoridges are 100 μm. Scale bar: 20 μm

standard deviations (STDs) smaller than 15 nm. This result shows that this Si nanomold fabrication method can produce uniform nanoridge structures. The bottom part of the silicon mold turned out to be wider compared to the top part after the LOCOS process. This was mainly due to the isotropic oxidation at the corner of the silicon nanoridge, and it affected the size of the top part of the formed nanochannel after nanoimrpinting (Chen et al. 2007). If needed, aspect ratio higher than 1:5.5 can also be achieved by reducing the pattern widths on the photomask or by carefully controlling the LOCOS process time. Figure 3c shows that the resulting sidewalls of the silicon nanoridges had low surface roughness owing to the anisotropic KOH etching along the silicon crystalline geometry when compared with other Si etching technique such as deep reactive ion etching (DRIE) (Chen et al. 2007; Liang et al. 2007). Generally, DRIE leaves sidewalls with corrugation or scallop shapes, because of the nature of the process sequence that is cycled between etching and passivation phases (Nilsson et al. 2003).

The nanoridges shown in Fig. 3d have different widths (200, 250, 300, 350, 400 and 450 nm), determined by the original photoresist pattern widths for Si_3N_4 etching (Fig. 1b). Thus, in a single device, it was possible to fabricate nanochannel arrays having different widths from micrometer scale patterns.

3.2 Nanoimprint lithography and nanochannel sealing using solvent vapor

Figure 4 shows a microscopy image and SEM images of imprinted PMMA nanotrench arrays (240 nm wide, 1.1 μm deep). The distance between trenches was 20 μm and the length was over 1 cm. The yield for the PMMA trench fabrication by imprinting was almost 100% for channels with aspect ratios under 1:5 ($n = 450$). However, for

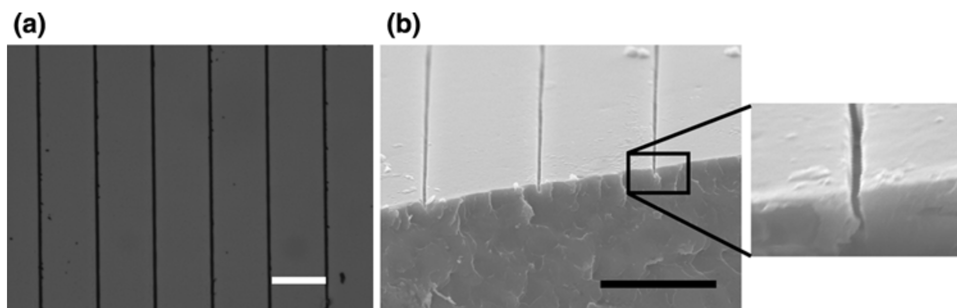

Fig. 4 Arrays of PMMA nanotrenches after nanoimprinting. **a** A microscopy image and **b** an SEM image showing PMMA nanotrenches having width and height of 240 nm and 1.1 μm, respectively. Scale bar: 20 μm

aspect ratios over 1:10 ($n = 50$), the silicon nanomolds were easily broken when the mold was separated from the PMMA substrate after imprinting. PMMA nanotrench width, measured at the top (240 nm), was 40 nm wider than the top part of the imprint mold (200 nm), due to the wider shape of the bottom part of the Si mold as shown in inset of Fig. 3a. The cross-sectional area on the SEM image (Fig. 4b) was not clean because the PMMA substrate was cut in liquid nitrogen by manually bending the sample for SEM imaging. The PMMA substrate was cut in liquid nitrogen in order to minimize the bending and stretching of the substrate during the cutting process, and no noticeable changes in trench geometry was observed after the process.

Figure 5 shows SEM images of a sealed nanochannel after applying toluene vapor for 10 s. Figure 5a shows the top surface of a sealed PMMA nanochannel after the process, and it can be seen that trenches have been uniformly sealed while the nanotrench track remaining still visible. Owing to the HAR trench geometry, only the topside of the trench was affected by toluene vapor and was sealed. This resulted in a nanoscale space at the bottom of the nanotrench (Fig. 5b, 240 nm wide, 1.1 μm high). No changes in channel widths were observed after the solvent-assisted sealing step. When the imprinted PMMA nanotrenches were exposed to solvent vapor for too long (>30 s), solvent vapor liquefied on the surface of the PMMA substrate and resulted in major damages to the patterns, and the nanochannel structures were no longer recognizable. If PMMA patterns were positioned too far away (>10 cm) from the solvent surface, PMMA patterns remained mostly unchanged with the nanotrenches still open. This is probably due to solvent vapor not sufficiently reaching the PMMA substrate. Also, when the aspect ratio was smaller than 2 (e.g. 500 nm wide and 1 μm high channel), this solvent-assisted sealing method failed to seal the trenches and only edges of the nanotrenches were melted by the solvent vapor (Fig. 5c).

The interaction of solvent systems (liquid or vapor at room temperature or at elevated temperature) with plastic

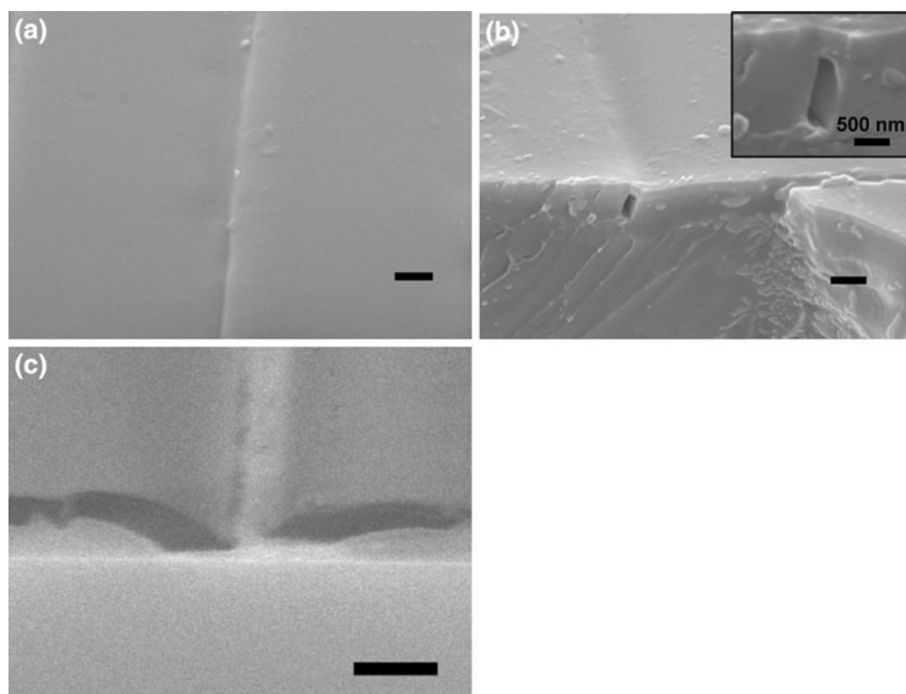

Fig. 5 SEM images of a PMMA nanochannel after solvent-assisted sealing. **a** Top-side view and **b** cross-sectional view of a sealed nanochannel. **c** A nanotrench not properly sealed due to an aspect ratio of smaller than 2. Width and height of the PMMA nanochannel was 240 nm and 1.1 μm, respectively. Scale bar: 2 μm

materials for their cleaning, polishing or other apparent surface property enhancements are well known (McGinniss 1985). This technique requires maintaining the temperature of the solvent above its boiling point but below the melting point of the PMMA during the sealing process. Other solvent systems are currently being investigated for this PMMA nanotrench sealing process for optimum result.

Surface properties and optical properties are important parameters for nanofluidic channels to be used in biosensing and bioanalysis applications. Surface properties of PMMA after the fabrication steps were characterized by measuring the contact angle of a water droplet on the surface. Ten micro liters of deionized water droplet was dispensed on the PMMA surface and the contact angle was measured using an optical tensiometer (Cam100, KSV Instruments, Helsinki, Finland). Measured contact angle of the Si substrate having spin-coated PMMA resist on it (M.W. 75,000) changed from 74.16° ± 0.44° to 79.87° ± 6.67° after the NIL process. The contact angle of PMMA plates changed from 76.34° ± 0.87° to 84.14° ± 1.55°. These analyses show that no issues are expected for the capillary action, which allows the DNA molecules to go into the PMMA nanochannel together with the solution. This was further confirmed by loading DNA tagged with SYBR Gold fluorescent dye (Invitrogen, Carlsbad, CA) into our fabricated nanochannels, as shown in Fig. 6. For low ionic strength solutions where the Debye length λ_D (0.1–10 nm for a concentration ranging from 0.1 to 10 mM) becomes comparable to the nanochannel size, repulsive electrostatic interactions between negatively charged biomolecules and like-charged nanochannel walls become prominent (Fu et al. 2007). Larger molecules unfold, decreasing their entropy in order to enter a channel slightly smaller than their diameter of gyration. The chain is trapped outside the constriction where it maximizes its conformational entropy (entropic trapping) (Han and Craighead 2000). Therefore, in this article, we believe that the electric charge or electrostatic interaction can be ignored and that the capillary force is the dominant force allowing DNA molecules to go into the nanochannels.

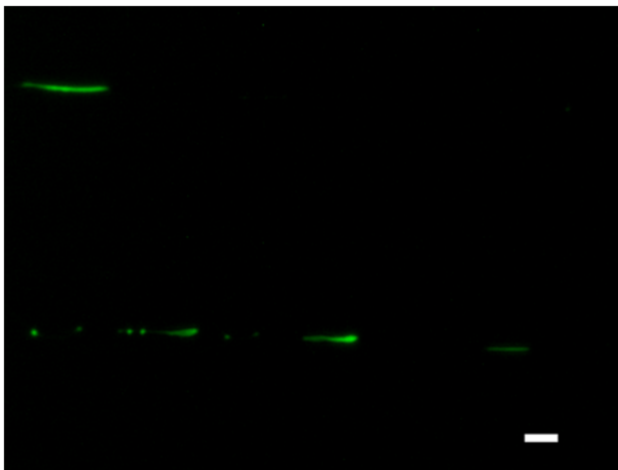

Fig. 6 A fluorescent microscopic image of SYBR Gold tagged DNA stretched inside two solvent-sealed PMMA nanochannels. Scale bar: 4 μm

Many of the biosensing and bioanalysis applications utilize fluorescent imaging/sensing, hence optical properties of PMMA are also important. The refractive indices of the PMMA used here were 1.48–1.50, and had a transmission property of >92% at wavelengths of 537 nm, the maximum emission wavelength for SYBR Gold fluorescent dye, therefore making these PMMA nanochannels suitable for DNA analysis applications.

Having nanochannels with various widths on a single device can greatly benefit biomolecular studies such as studying DNA stretching behavior in nanochannels by significantly reducing the time and cost required for such experiments. Guo et al. (2004) showed the relationship between nanochannel sizes and the degree of DNA molecule stretching inside nanochannels. When a DNA molecule is forced to flow through a nanochannel having a cross section comparable to the radius of gyration of DNA, it is energetically more favorable for the DNA molecules to be in the stretched states. Evaluating and understanding DNA behavior and stretching state require significant amount of experiments with nanochannels having various width for conditions such as ion concentration in buffer solution and intercalating dye concentration. Another advantage of this fabrication technique is the easy and low cost sealing of nanotrenches using solvent vapor, without requiring the typically used but more costly sputtering or e-beam evaporation method. This also results in an all-polymer nanochannel array. By using the developed technique to create nanochannels with various widths on a single device, the pace of such studies can be greatly accelerated.

4 Conclusions

We present a simple and low cost method of fabricating high aspect ratio (HAR) polymer nanochannels without the use of expensive nanofabrication tools. The HAR silicon nanoimprint mold fabrication process is based on the combination of anisotropic etching of silicon by potassium hydroxide (KOH) solution and local oxidation of silicon (LOCOS). The widths of the nanoimprint molds were easily controllable (200–500 nm) by the initial microscale photoresist patterns and the oxidation time, making this fabrication process a simple and practical solution for low cost and high-throughput fabrication of HAR silicon nanoimprint mold. To create nanochannels out of these nanotrenches, a novel solvent-assisted sealing technique

was developed in order to seal the HAR PMMA nanotrenches. Using this fabrication method, nanochannels that were 200–500 nm wide, 1.1 μm deep, and more than 1 cm long were successfully fabricated. This technique enables the generation of nanochannels with various nanoscale dimensions at low cost, and has the potential for mass fabrication of nanofluidic devices.

Acknowledgments This work was supported by the Practical Application Project of Advanced Microsystems Packaging Program of Seoul Technopark, funded by the Korean Ministry of Knowledge Economy (Grant # 10029790).

References

Abgrall P, Nguyen NT (2008) Nanofluidic devices and their applications. Anal Chem 80:2326–2341

Bai JG, Chang CL, Chung JH, Lee KH (2007) Shadow edge lithography for nanoscale patterning and manufacturing. Nanotechnology 18:405307

Bai JG, Yeo WH, Chung JH (2009) Nanostructured biosensing platform-shadow edge lithography for high-throughput nanofabrication. Lab Chip 9:449–455

Cao H, Yu ZN, Wang J, Tegenfeldt JO, Austin RH, Chen E, Wu W, Chou SY (2002) Fabrication of 10 nm enclosed nanofluidic channels. Appl Phys Lett 81:174–176

Chen LQ, Chan-Park MB, Yan YH, Zhang Q, Li CM, Zhang J (2007) High aspect ratio silicon nanomoulds for UV embossing fabricated by directional thermal oxidation using an oxidation mask. Nanotechnology 18:355307

Cho YH, Lee SW, Kim BJ, Fujii T (2007) Fabrication of silicon dioxide submicron channels without nanolithography for single biomolecule detection. Nanotechnology 18:465303

Chou SY, Krauss PR, Renstrom PJ (1996) Imprint lithography with 25-nanometer resolution. Science 272:85–87

Craighead HG (2006) Future lab-on-a-chip technologies for interrogating individual molecules. Nature 442:387–393

Dumond JJ, Low HY, Rodriguez I (2006) Isolated, sealed nanofluidic channels formed by combinatorial-mould nanoimprint lithography. Nanotechnology 17:1975–1980

Fu J, Schoch RB, Stevens AL, Tannenbaum SR, Han J (2007) A patterned anisotropic nanofluidic sieving structure for continuous-flow separation of DNA and proteins. Nat Nanotechnol 2:121–128

Grabiec PB, Zaborowsk M, Domansik K, Gotszalk T, Rangelow IW (2004) Nano-width lines using lateral pattern definition technique for nanoimprint template fabrication. Microelectron Eng 73–74:599–603

Guo LJ, Cheng X, Chou CF (2004) Fabrication of size-controllable nanofluidic channels by nanoimprinting and its application for DNA stretching. Nano Lett 4:69–73

Han J, Craighead HG (2000) Separation of long DNA molecules in a microfabricated entropic trap array. Science 288:1026–1029

Haneveld J, Berenschot E, Maury P, Jansen H (2006) Nano-ridge fabrication by local oxidation of silicon edges with silicon nitride as a mask. J Micromech Microeng 16:S24–S28

Huh D, Mills KL, Zhu X, Burns MA, Thouless MD, Takayama S (2007) Tuneable elastomeric nanochannels for nanofluidic manipulation. Nat Mater 6:424–428

Jo K, Dhingra DM, Odijk T, de Pablo JJ, Graham MD, Runnheim R, Forrest D, Schwartz DC (2007) A single-molecule barcoding system using nanoslits for DNA analysis. Proc Natl Acad Sci USA 104:2673–2678

Langford RM, Nellen PM, Gierak J, Fu YQ (2007) Focused ion beam micro- and nanoengineering. MRS Bull 32:417–423

Liang X, Morton KJ, Austin RH, Chou SY (2007) Single sub-20 nm wide, centimeter-long nanochannel fabricated by novel nanoimprinting mold fabrication and direct imprinting. Nano Lett 7:3774–3780

Mannion JT, Reccius CH, Cross JD, Craighead HG (2006) Conformational analysis of single DNA molecules undergoing entropically induced motion in nanochannels. Biophys J 90:4538–4545

McGinniss VD (1985) Vaporous solvent treatment of thermoplastic substrates. United States Patent 4529563

Mikayama T, Suzuki T, Matsui J, Miyashita T (2005) Fabrication of depth-controllable nanochannel with polymer nanoassembled films using atomic force microscopy lithography. Polym J 37:854–857

Nilsson D, Jensen S, Menon A (2003) Fabrication of silicon molds for polymer optics. J Micromech Microeng 13:S57–S61

Nishino T, Meguro M, Nakamae K, Matsushita M, Ueda Y (1999) The lowest surface free energy based on -CF3 alignment. Langmuir 15:4321–4323

Perry JL, Kandlikar SG (2006) Review of fabrication of nanochannels for single phase liquid flow. Microfluid Nanofluid 2:185–193

Reano RM, Pang SW (2005) Sealed three-dimensional nanochannels. J Vac Sci Technol B 23:2995–2999

Riehn R, Lu MC, Wang YM, Lim SF, Cox EC, Austin RH (2005) Restriction mapping in nanofluidic devices. Proc Natl Acad Sci USA 102:10012–10016

Tamaki E, Hibara A, Kim HB, Tokeshi M, Kitamori T (2006) Pressure-driven flow control system for nanofluidic chemical process. J Chromatogr A 1137:256–262

Tegenfeldt JO, Prinz C, Cao H, Reisner WW, Riehn R, Wang YM, Cox EC, Sturm JC, Silberzan P, Austin RH (2004) The dynamics of genomic-length DNA molecules in 100-nm channels. Proc Natl Acad Sci USA 101:10979–10983

Vangbo M, Backlund Y (1996) Precise mask alignment to the crystallographic orientation of silicon wafers using wet anisotropic etching. J Micromech Microeng 6:279–284

Wang KG, Yue S, Wang L, Jin A, Gu C, Wang P, Wang H, Xu X, Wang Y, Niu H (2006) Manipulating DNA molecules in nanofluidic channels. Microfluid Nanofluid 2:85–88

Zaborowsk M, Szmigiel D, Gotszalk T, Ivanova K, Sarov Y, Volland BE, Rangelow IW, Grabiec P (2006) Nano-line width control and standards using lateral pattern definition technique. Microelectron Eng 83:1555–1558

Zhao Y, Berenschot E, de Bore M, Jansen H, Tas N, Huskens J, Elwenspoek M (2008) Fabrication of a silicon oxide stamp by edge lithography reinforced with silicon nitride for nanoimprint lithography. J Micromech Microeng 18:064013